Time-dependent universal conductance fluctuations and coherence in AuPd and Ag

A. Trionfi, S. Lee, and D. Natelson
Department of Physics and Astronomy, Rice University, 6100 Main Street, Houston, Texas 77005, USA
(Received 29 September 2004; revised manuscript received 16 March 2005; published 5 July 2005)

Quantum transport phenomena allow experimental assessment of the phase coherence information in metals. We report quantitative comparisons of coherence lengths inferred from weak localization magnetoresistance measurements and time-dependent universal conductance fluctuation data. We describe these two measurements and their analysis. Strong agreement is observed in both quasi-two-dimensional and quasi-one-dimensional (1D) AuPd samples, a metal known to have high spin-orbit scattering. However, quantitative *disagreement* is seen in quasi-1D Ag wires below 10 K, a material with intermediate spin-orbit scattering. We consider explanations of this discrepancy, with particular emphasis on the theoretical expressions used to analyze the field dependence of the conductance fluctuations. We also discuss the mechanism of the suppression of conductance fluctuations at high drive levels, and dephasing mechanisms at work in these systems.

DOI: 10.1103/PhysRevB.72.035407 PACS number(s): 73.23.−b, 73.50.−h, 72.70.+m, 73.20.Fz

I. INTRODUCTION

Quantum phase coherence in normal metals gives rise to numerous corrections to the classically predicted conductivity. These corrections are commonly referred to as quantum transport phenomena (QTP). The study of QTP has both fundamental physical importance[1] and possible implications in novel device architectures.[2,3] The typical experimental application of QTP is to infer quantum coherence time and length scales. Weak localization magnetoresistance (WL),[4] magnetic field-dependent universal conductance fluctuations[5,6] (MFUCF), time-dependent universal conductance fluctuations[7,8] (TDUCF), and Aharonov-Bohm oscillations[9] have all been used to examine coherence in normal metals.

QTP in diffusive conductors arise due to an interference between possible electronic trajectories from one location to another. Interference, however, is only relevant when the phase of the conduction electrons' partial waves is well-defined. The coherence length is defined as the distance scale over which the phase of a conduction electron's wave function remains correlated to its initial phase. This length can be related to a coherence *time*, τ_ϕ, by $L_\phi = \sqrt{D\tau_\phi}$ where D is the diffusion constant of the electron in the disordered solid. Decoherence or dephasing can occur when an electron experiences an interaction with another dynamical degree of freedom. The three most common dephasing processes are electron-electron scattering, electron-phonon scattering, and spin-flip interactions with magnetic impurities. The rates of these processes have distinct temperature dependences, allowing QTP to be used to distinguish between these mechanisms in various metals.

Interesting questions have arisen from experimental characterization of electron coherence. One question is whether precisely the same coherence length is inferred from different QTP. This is a subtle issue because the precise time scales and processes relevant to a particular observable can be complicated, and the evolution of electronic phase correlations is typically not a simple single-time exponential decay. A previous test of this coherence length consistency led to equivocal results in quasi-two-dimensional (2D) silver.[10] Another question is the cause of an observed low temperature saturation of the coherence length in many materials.[11] An explanation with significant experimental support is scattering from dilute concentrations of low Kondo temperature magnetic impurities,[12] while others suggest intrinsic mechanisms.[13] These two questions are increasingly related: Recent publications[14,15] have compared experimental results from different QTP when debating the cause of coherence saturation; it must be established, however, that these analyses are truly comparing equivalent parameters.

In this paper we briefly review the physics underlying WL, MFUCF, and TDUCF, and report measurements of these effects in two different materials, $Au_{0.6}Pd_{0.4}$ and Ag, over a broad temperature and field range. While we find excellent quantitative agreement between $L_\phi^{WL}(T)$ and $L_\phi^{TDUCF}(T)$ in all AuPd samples, we observe a *divergence* between these two inferred coherence lengths in quasi-one-dimensional (1D) Ag samples, as seen previously in quasi-2D Ag films.[10] We discuss candidate explanations and suggest that a likely concern is the applicability of the theoretical expressions used to analyze the TDUCF field dependence. We also show that the suppression of TDUCF amplitude at high drive currents is consistent with bias-induced energy averaging. Finally we discuss the implications of these data on dephasing mechanisms at work in these systems.

Weak localization arises from the properties of electronic trajectories under time-reversal symmetry. Many electronic paths in a diffusive conductor contain loops. Without a magnetic field, an electron circumnavigating such a loop accumulates the same phase as one doing so under time-reversed conditions. This phase agreement causes constructive interference that enhances backscattering, leading to a conductivity lower than is classically predicted. With strong spin-orbit interactions, the sign of this interference is reversed and leads to enhanced conduction. In the presence of a magnetic field normal to the loop, the vector potential adds opposite phase shifts to each looped path and corresponding time-reversed conjugate. This eliminates the constructive (destructive) interference when ~ one quantum of flux is threaded

through a typical loop. The result is a magnetoresistance with a field scale related to the area of a typical coherent loop, allowing inference of L_ϕ^{WL}.

Time-dependent UCF are due to the enhanced sensitivity of the conductance to the motion of individual scatters. Unlike weak localization, all interfering paths contribute to this phenomenon. When a scattering site moves, it changes the interference pattern of all intersecting electronic paths within a coherent volume of the scattering site, leading to a conductance change. A single moving scatter can change the conductance within a coherent volume at zero temperature by roughly e^2/h. If the relaxation times of the scatters are appropriately distributed, the TDUCF exhibit a $1/f$ power spectrum,[16] which is the case in many normal metals. Much like weak localization, the noise power of the $1/f$ noise is sensitive to a perpendicular magnetic field. The time-reversed loop contribution (the cooperon) will be suppressed as the field is increased while the sensitivity due to all remaining paths, known as the diffuson, remain unchanged.[17] This leads to a factor of 2 decrease in the noise power as the field is ramped up, and allows extraction of L_ϕ^{TDUCF}.

Magnetic field-dependent UCF are closely related to the time-dependent form. The explanation of this phenomenon comes from the ergodic hypothesis,[18,19] which implies that other effects that randomize the interference of electronic paths are equivalent to scattering site motion. Since a perpendicular magnetic field introduces an Aharonov-Bohm phase shift particular to each electronic path, varying such a field leads to conductance fluctuations of the universal size of $\sim e^2/h$. The result is a completely reproducible magnetoresistive pattern that is sample-specific, commonly referred to as the magnetofingerprint.

Although the expected size of the conductance fluctuations is universal, the measured effect may be much smaller. Samples much longer and wider than L_ϕ may be treated as uncorrelated fluctuators in series and parallel. The measured noise power is therefore reduced by a factor N, the number of coherent volumes between the ends of the measured sample. Further averaging occurs when the energy range of accessible single-particle states exceeds the correlation energy,[20] $E_c=\hbar D/L_\phi^2$. In this case the relevant states can be subdivided by energy into coherent subbands, each nominally uncorrelated with the others, leading to further ensemble averaging. One way to increase available energy levels is via thermal energy. The thermal length, $L_T \equiv (\hbar D/k_B T)^{1/2}$, is the distance two initially in-phase electrons separated in energy by $k_B T$ may move before their phases differ by ~ 1. The condition $L_T < L_\phi$ is equivalent to $k_B T > E_c$, leading to ensemble averaging by L_T/L_ϕ to some power. Similarly, when $eV_c > E_c$, where V_c is the voltage dropped across a coherence length, ensemble averaging will also occur.[6]

The observed magnitude of the TDUCF may also be smaller than the universal limit if the conductance fluctuations are not "saturated." A sample is said to be in the saturated regime if the conductance variance within a coherent volume has reached the limiting $\sim e^2/h$ amplitude. How close a sample is to this condition depends on the microscopic nature of the fluctuators. Since MFUCF should always exhibit conductance fluctuations on order e^2/h within a coherent volume, if a sample is in the saturated regime, the TDUCF noise power integrated over the bandwidth of the fluctuators should equal the MFUCF magnitude. That is, $\int_0^\infty S_G(f)df$ should equal $(\delta G^{\mathrm{MFUCF}})^2$, where S_G is the conductance noise power, f is the frequency, and G is the conductance. If the fluctuators are typical tunneling two-level systems (TLS) of the type ubiquitous in disordered solids,[21] their relaxation rates are estimated to span ~ 20 decades.[7] TDUCF measurements in the literature are all thought to be nonsaturated. This issue is important, as it determines the functional form appropriate for analysis of the field dependence of the TDUCF.

For WL and TDUCF, the number of the sample dimensions longer than L_ϕ determines the effective dimensionality of the system with regard to coherence effects. Thus a quasi-2D sample is achieved when $t \ll L_\phi \ll w$ and a quasi-1D sample when $w, t \ll L_\phi$. Here t and w are sample thickness and width, respectively.

Previous comparisons between $L_\phi^{\mathrm{WL}}(T)$ and $L_\phi^{\mathrm{TDUCF}}(T)$ have shown a disagreement between these parameters at low temperatures in quasi-2D Ag samples.[10] This was interpreted as evidence supporting a theoretical treatment[22] that argued that the Nyquist or electron-electron dephasing rate would limit the coherence in WL while the out-scattering rate would limit the coherence in universal conductance fluctuations. The out-scattering rate is the rate at which an electron will change its momentum state in the Boltzmann formalism. It was shown the two rates have different temperature dependencies at low temperature so a divergence between the coherence lengths inferred from WL and TDUCF was expected. Recent corrections to the theory[23] show that, as long as electron-electron scattering is the only small-energy-transfer inelastic process, L_ϕ^{WL} is expected to equal L_ϕ^{TDUCF}. This leaves the experimental results in Ag without an explanation. We discuss this further below.

II. PROCEDURE

Samples were patterned on undoped GaAs substrates using standard electron beam lithography, as discussed in Ref. 24. Distances between consecutive leads (voltage or current) were 10 μm in AuPd samples and 20 μm in Ag samples. Ag (0.99999 purity) samples were made using a single lithography/deposition step with the wire and leads all silver, and no adhesion layer. $Au_{0.6}Pd_{0.4}$ samples were made using two lithography steps, the first for the AuPd wire and the second for the Ti/Au leads (1.5 nm Ti, 25 nm Au). The AuPd source material is expected to be free of ferromagnetic impurities to the 10^{-5} level. To minimize the contact resistance between the AuPd wires and the Ti/Au leads, samples were exposed to oxygen plasma for 30 s prior to the Ti/Au deposition to remove any resist residue. Typical contact resistances in the AuPd samples were less than 30 Ω. All depositions were performed using an electron beam evaporator at 5×10^{-7} mB. To test the effects of magnetic impurities on the consistency of L_ϕ^{WL} and L_ϕ^{TDUCF}, one AuPd sample was deliberately contaminated with trace impurities by evaporating 2.5 nm of $Ni_{0.8}Fe_{0.2}$ with the sample shutter *closed*, prior to the AuPd evaporation.

Measurements between 2 and 20 K were performed in a ^{4}He cryostat while lower temperatures for two samples (G,H) were achieved in a dilution refrigerator. All samples were initially characterized with standard ac four terminal resistance measurements and tested as a function of temperature at various drive currents to check for Joule heating. Upturns in the resistance at low temperatures were consistent with electron-electron interaction corrections. All subsequent measurements were performed at or below the limiting current set by the Joule heating tests.

WL magnetoresistance measurements were made using standard four terminal techniques. The applied field was swept between ±1.25 T for AuPd samples while the field range for the Ag samples was ±0.9 T. The TDUCF measurement employed an ac five terminal bridge technique developed by Scofield.[25] The ac bridge technique renders the noise measurement insensitive to noise in the voltage source. The bridge was measured with a low noise differential preamplifier (1.2 nV/$\sqrt{\text{Hz}}$, NF Electronics LI-75A). Signal frequencies ranged from 600 Hz for AuPd samples to 1 kHz for Ag samples, chosen to optimize the noise contours of the preamplifier. Both the in-phase and out-of-phase demodulated signals were fed into a two-channel dynamic signal analyzer (SRS SR785) to transform the data into the frequency domain. Strong $1/f$ dependent spectra were consistently observed from the in-phase channel while the out-of-phase channel provided a measure of the white background noise of the measurement circuit. By subtracting away this background, the sample-induced noise could be isolated. A typical frequency span ranged from 78 mHz to 1.5 Hz for the AuPd samples and to 3 Hz in Ag samples. The low temperature noise power in all samples show the expected amplitude increase with decreasing temperature as well as the factor of 2 drop in the presence of a large perpendicular magnetic field (except when local interference noise becomes nonnegligible). This observation is consistent with the expected TDUCF behavior.

The bridge technique was also employed to make the MFUCF measurements. By using this method instead of the standard four terminal resistance measurement, the WL magnetoresistance is nulled away since both sides of the bridge will have identical resistance changes due to this effect. The nulling of the WL magnetoresistance allows the magnetofingerprint to be observed down to zero field. An example of the magnetofingerprint is given in Fig. 1.

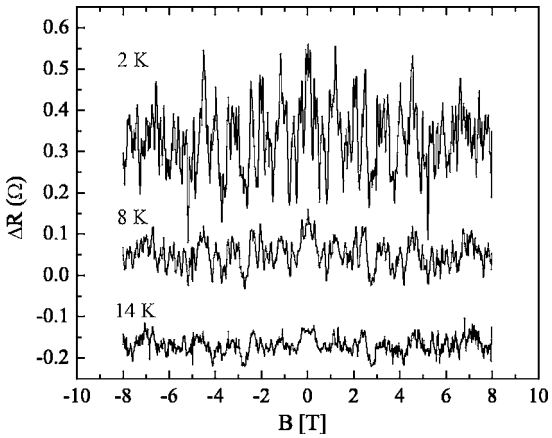

FIG. 1. "Magnetofingerprint" measurements on sample I made using the five terminal bridge technique. The curves from top to bottom are at 2, 8, and 14 K. The curves are offset for clarity.

III. ANALYTICAL APPROACH

A. Weak localization

Values of L_ϕ^{WL} were inferred from the AuPd WL magnetoresistance using the following equations for one and two dimensions, respectively:[12,26]

$$\left.\frac{\Delta R}{R}\right|_{\text{1D}} = -\frac{e^2}{2\pi\hbar}\frac{R}{L}\left[\frac{1}{L_\phi^2}+\frac{1}{12}\left(\frac{w}{L_B^2}\right)^2\right]^{-1/2}, \tag{1}$$

$$\left.\frac{\Delta R}{R}\right|_{\text{2D}} = \frac{e^2}{4\pi^2\hbar}R_\square\left[\psi\left(\frac{1}{2}+\frac{1}{2}\frac{L_B^2}{L_\phi^2}\right)-\ln\left(\frac{1}{2}\frac{L_B^2}{L_\phi^2}\right)\right], \tag{2}$$

ψ is the digamma function and $L_B \equiv \sqrt{\hbar/2eB}$. $R_\square$ is the sheet resistance of the sample, R is $R(B=\infty)$, w is the sample dimension transverse to both the applied field and current flow, and L is the length of the sample parallel to current flow. These equations apply in the limit of *strong* spin-orbit scattering ($\tau_{\text{SO}} \ll \tau_\phi$). AuPd has long been established as a strong spin-orbit scattering material.[26]

The L_ϕ^{WL} values inferred from the quasi-1D Ag wires used the more general form,[12]

$$\left.\frac{\Delta R}{R}\right|_{\text{1D}} = -\frac{e^2}{2\pi\hbar}\frac{R}{L}\left[3\left(\frac{1}{L_\phi^2}+\frac{4}{3L_{\text{SO}}^2}+\frac{1}{12}\left(\frac{w}{L_B^2}\right)^2\right)^{-1/2} - \left(\frac{1}{L_\phi^2}+\frac{1}{12}\left(\frac{w}{L_B^2}\right)^2\right)^{-1/2}\right]. \tag{3}$$

Here $L_{\text{SO}} \equiv \sqrt{D\tau_{\text{SO}}}$ is the spin-orbit length. ΔR for Eq. (2) is defined as $\Delta R = R(B) - R(B=0)$, while it is defined as $\Delta R = R(B) - R(B=\infty)$ in Eqs. (1) and (3). The only fitting parameter for the AuPd curves is L_ϕ, while both L_ϕ and L_{SO} are free in the fits for the Ag curves. The width is left free at 2 K in all one-dimensional fits to confirm sample size and is then fixed for all subsequent fits. Spin-orbit lengths are also fixed above 10 K to the average value found from lower temperature fits.

B. TDUCF noise

L_ϕ^{TDUCF} values were inferred from fits of the noise power as a function of perpendicular field to the appropriate crossover function, $\nu(B)$, the theoretically expected functional form. There are two methods of calculating $\nu(B)$; we have used both approaches and compared the results. First, analytical expressions for the one-dimensional and two-dimensional crossover functions with large spin-orbit interaction have been derived recently by Aleiner:[27]

$$\nu_{\text{1D}}(B) = 1 - \frac{x}{2}\left(\frac{\text{Ai}(x)}{\text{Ai}'(x)}\right)^2, \tag{4}$$

where $x \equiv L_\phi^2/[3(\hbar/Bew)^2]$, and

$$\nu_{2D}(B) = \frac{1}{2} + \frac{L_B^2}{4L_\phi^2}\psi'\left(\frac{1}{2} + \frac{L_B^2}{2L_\phi^2}\right). \quad (5)$$

These functional forms are strictly valid when $\hbar/\tau_\phi \ll k_B T$. Here $\mathrm{Ai}(x)$ is the Airy function, and $\psi'(x)$ is the derivative of the digamma function.

Prior to the derivation of these analytical results, the noise crossover function was calculated from the theoretical expression for the magnetic field correlation function $F(\Delta E, \Delta B, B) \equiv \langle \delta g(E_F, B)\delta g(E_F+\Delta E, B+\Delta B)\rangle$ of the MFUCF.[17,28,29] Here g is the conductance in units of e^2/h. An approximation of this correlation function has been derived by Beenakker and van Houten[30] for quasi-1D samples. We also analyze the data with this method and compare with the analytical expressions above. The samples are assumed to be in the unsaturated regime, so that the derivative of F with respect to τ_ϕ^{-1} must be computed, as per the explanation given by Stone.[17] The resulting derivative has the form

$$F'(B) = \frac{L_{\phi B}^5\left(1 + \frac{3L_{\phi B}^2(B)}{2\pi L_T^2}\right)}{\left(1 + \frac{9L_{\phi B}^2(B)}{2\pi L_T^2}\right)}, \quad (6)$$

where

$$L_{\phi B}^2(B) = \frac{3L_\phi^2}{(BeL_\phi w/\hbar)^2 + 3}. \quad (7)$$

Spin-orbit interactions may be accomodated by changing Eq. (6) to[31]

$$F'(B) = \frac{L_{\phi B}^5\left(1 + \frac{3L_{\phi B}^2(B)}{2\pi L_T^2}\right)}{4\left(1 + \frac{9L_{\phi B}^2(B)}{2\pi L_T^2}\right)} + \frac{3L_{\phi Bt}^5\left(1 + \frac{3L_{\phi Bt}^2(B)}{2\pi L_T^2}\right)}{4\left(1 + \frac{9L_{\phi Bt}^2(B)}{2\pi L_T^2}\right)}, \quad (8)$$

where

$$L_{\phi Bt}^2(B) = \frac{3L_\phi^2 L_{SO}^2}{(BeL_\phi L_{SO} w/\hbar)^2 + 3L_{SO}^2 + 4L_\phi^2}. \quad (9)$$

The approximate crossover function is therefore

$$\nu(B) = \frac{1}{2} + \frac{F'(B)}{2F'(B=0)}. \quad (10)$$

The exact crossover function in quasi-2D systems was reported by Stone[17] and was also used to infer L_ϕ^{TDUCF} in the quasi-2D AuPd samples. The fitting method employed was that described in Ref. 32. A comparison between the crossover functions computed from the correlation functions and the analytic expressions of Eqs. (4) and (5) finds the following results. In the quasi-1D case, the L_ϕ^{TDUCF} values inferred using the correlation functions systematically exceed those extracted using the analytical expressions by roughly 10%. Similarly, in the quasi-2D case, the correlation function-based values exceed those from Eq. (5) by 3%.

The actual fitting functions used to analyze the normalized noise power data included an additional fitting parameter to account for the local interference noise[33–35] that increases to non-negligible magnitudes at higher temperatures. Since local interference noise has no low order field dependence, the noise power will not drop by a full factor of 2 at higher temperatures. The corrected fitting function has the form $f(B) = (1-z) + z\nu(B)$ where z represents the fractional size of the UCF enhanced noise. Values of z were indistinguishable from 1 for all data sets except at 20 K in the quasi-2D AuPd samples and quasi-1D Ag samples. All fitting was performed using standard χ^2 minimization.

C. Role of magnetic impurity scattering

As was discussed extensively in Ref. 12, magnetic impurity scattering can affect weak localization and UCF coherence corrections *differently* or *identically* depending on the temperature scale and impurity concentration. At temperatures higher than a crossover temperature, the Korringa time for impurity spins to relax back to thermal equilibrium with the lattice is short compared to the spin-flip scattering time. In this regime ($T > T^* \equiv \sim 40$ mK$\times$ the ppm concentration of magnetic impurities for typical host noble metals), spin-flip scattering should involve large energy transfers[27] and affect WL and TDUCF *identically*. At temperatures below this cutoff, spin scattering is more rapid than the relaxation of the impurity spins; under these conditions, the spin-flip scattering time is predicted to affect TDUCF and WL *differently*.

An estimate of the decoherence rate due to magnetic impurities may be obtained from the Nagaoka-Suhl expression:[36]

$$\frac{1}{\tau_{sf}} = \frac{c_{mag}}{\pi\hbar\nu(E_F)}\frac{\pi^2 S(S+1)}{\pi^2 S(S+1) + \ln^2(T/T_K)}, \quad (11)$$

where $\nu(E_F)$ is the density of states at the Fermi level of the host metal, S is the spin of the impurity, and T_K is the Kondo temperature of the impurity in the host metal.

IV. RESULTS AND DISCUSSION

Magnetoresistance curves for both AuPd and Ag samples are given in Fig. 2. The data are fit very well by Eqs. (1)–(3). Sample widths inferred for the quasi-1D wires via the fitting procedure are consistent with SEM images and estimates based on resistances of codeposited films. Including L_{SO} as a fit parameter in the AuPd data leads to $L_{SO} \lesssim 10$ nm, with little impact on L_ϕ. We find $L_{SO} \approx 290$ nm for Ag, and ~ 9 nm for AuPd.

Similarly, examples of the measured normalized noise power $[S_R(B)/S_R(B=0)]$ versus field are shown in Fig. 3 for sample F, a quasi-1D silver wire. As is clear from the graph, these data are fit well by the Beenakker/van Houten correlation function approach [Eq. (8) and following].

A. AuPd comparison of WL and TDUCF

Figure 4(a) shows the resulting coherence lengths inferred from both QTP for the two quasi-1D AuPd samples, as origi-

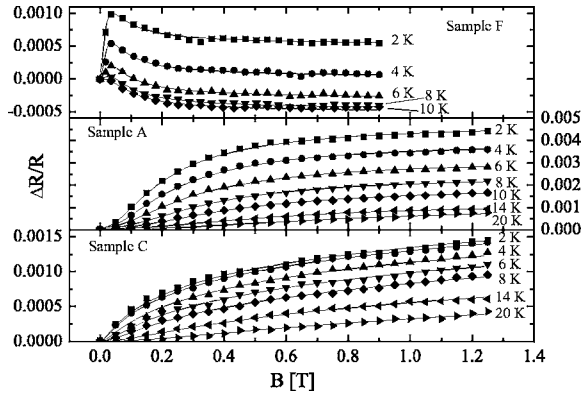

FIG. 2. WL magnetoresistance curves at various temperatures for a 43 and 500 nm AuPd wire (samples A and C) and a 140 nm Ag wire (sample F). Quasi-1D data shifted to pass through origin.

nally reported in Ref. 24. The inferred L_ϕ^{WL} and L_ϕ^{TDUCF} are in *strong quantitative agreement* for the AuPd samples over the temperature range measured.

As shown in Ref. 24, this agreement remains strong even in the presence of magnetic impurity scattering significant enough to suppress the coherence length by more than a factor of 2. This strongly supports the theoretical statement[23] that weak localization and UCF measurements probe *precisely* the same coherence physics, even in the presence of strong spin-orbit and magnetic impurity scattering over this temperature range. Furthermore, the agreement persists even though $\hbar/\tau_\phi$ is never $\ll k_B T$, suggesting that Eqs. (4) and (5) are robust even when that constraint is somewhat relaxed.

B. Ag comparison of WL and TDUCF

Figure 4(b) shows the equivalent $L_\phi(T)$ data for the Ag samples over the same temperature range. Note that $L_\phi^{\mathrm{WL}}(T)$ shows no saturation, and at low temperatures approaches the Nyquist predicted value with *no* adjustable parameters. This

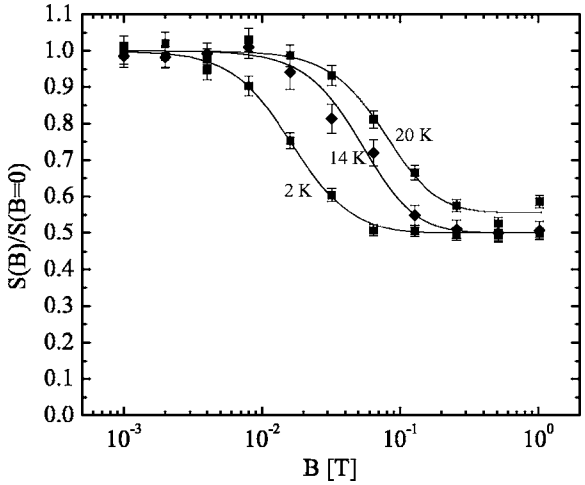

FIG. 3. Noise power data from Ag sample F at 2, 14, and 20 K. The crossover field becomes larger as the coherence length diminishes. The 20 K data do not drop by a full factor of 2 due to local interference noise.

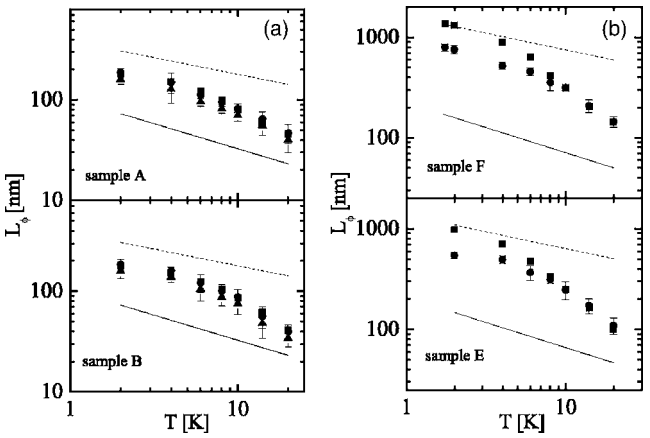

FIG. 4. (a) Coherence lengths as a function of T for the AuPd samples (lettered accordingly). Triangle points are inferred from Eq. (4), circles are inferred from Eq. (6), and squares are inferred from WL. Only one UCF fit is shown in quasi-2D since the two results only differ by 3%. The dashed lines show the predicted dephasing length due to Nyquist scattering calculated from sample parameters. The solid line represents the calculated thermal length. (b) Coherence lengths as a function of T for Ag samples E and F (lettered accordingly). Circle points are inferred from Eq. (8), and squares are inferred from WL. The dashed lines show the predicted dephasing length due to Nyquist scattering calculated from sample parameters. The solid line represents the calculated thermal length. Unlike the AuPd case, there is a statistically significant discrepancy between L_ϕ^{WL} and L_ϕ^{TDUCF} in these samples.

strongly suggests that *e-e* interactions are the only non-negligible dephasing mechanism in the Ag samples at temperatures near 2 K.

Comparing Fig. 4(b) with Fig. 4(a) highlights a dramatic difference between the Ag and AuPd data: There is substantial disagreement between L_ϕ^{WL} and L_ϕ^{TDUCF} in these quasi-1D Ag samples. In particular, below 8 K, L_ϕ^{TDUCF} is shorter and has a significantly weaker temperature dependence than $L_\phi^{\mathrm{WL}}(T)$. This difference is very similar to that observed previously in quasi-2D Ag films.[10]

The reason for this disagreement is unknown. A possibility put forward by Aleiner and Blanter is that a subtle effect due to triplet channel electrons is responsible.[23] This suggestion reflects the observation in the quasi-2D Ag data that the disagreement appears at temperatures below $L_\phi \approx L_{\mathrm{SO}}$. Our AuPd data, however, appear *inconsistent* with such an explanation. The inferred coherence lengths in a strong spin-orbit scattering material (AuPd) should resemble the low-temperature limiting behavior of a material with intermediate spin-orbit scattering (Ag). The WL/TDUCF agreement seen in the AuPd would imply that the coherence lengths inferred from the Ag should *agree* as the temperature is reduced. To the lowest temperatures measured, no such convergence is observed. A related prediction[27] would be for a signature of unusual triplet effects in $R(T)$ when $k_B T \lesssim \hbar/\tau_{\mathrm{SO}}$. Since $\tau_{\mathrm{SO}} \approx 3.5 \times 10^{-11}$ s, this crossover would be predicted at ~200 mK. No change in the $R(T)$ properties is observed down to 50 mK. TDUCF noise measurements at these lower temperatures have yet to be performed successfully and are very challenging due to Joule heating concerns. On the basis

of the AuPd data at hand, a triplet channel effect seems extremely unlikely to explain the differences between Figs. 4(a) and 4(b).

We suggest another possible resolution to this discrepancy between the AuPd and Ag data: the applicability of the noise crossover expressions used in analyzing the data. The two materials can be in different regimes (i.e., saturated vs unsaturated noise) at a fixed temperature, even if the distributions of TLS are identical, because of the different coherence lengths in AuPd and Ag. For given TLS properties, a minimum number of TLS must be present within each independent coherent volume to reach the saturated noise regime.[37] Even for identical TLS concentrations and properties, it is clear that the Ag would achieve this condition at a higher temperature due to its much longer coherence lengths (regardless of what sets the coherence length). There would be some crossover temperature where only some of the independent coherent volumes in a Ag sample show saturated conductance fluctuations; in this regime, neither the unsaturated nor the saturated crossover functions should be expected to fit the data well, and some interpolating formula would be necessary. In particular, if the Ag samples were transitioning into the saturated noise limit, then the fitting functions based on $F'(B)$ above used to infer the coherence length would be inappropriate. In the saturated limit, $F(B)$ rather than its derivative with respect to the inelastic rate is the correct function from which to derive $\nu(B)$.

Comparing the results of L_ϕ^{TDUCF} inferred using the saturated noise crossover function shows that incorrectly using the unsaturated noise crossover function will result in inferred coherence lengths less than the actual value. A comparison of integrated noise power amplitude to MFUCF resistance variances calculated from magnetofingerprint data confirms that the Ag noise is not yet saturated. The TDUCF noise in sample F would need to be integrated over 190 decades in frequency (completely unphysical) to achieve the conductance fluctuation size seen in MFUCF.

Figure 5 shows the results of trying to infer $L_\phi^{\mathrm{TDUCF}}(T)$ using the crossover function appropriate for saturated TDUCF, in comparison with the weak localization data and the L_ϕ^{TDUCF} values calculated using the unsaturated TDUCF expression. The large error bars in the saturated fits arise for two reasons: at larger values of the coherence length, the fit is more sensitive to small absolute errors in the magnitude of the crossover field; second, the functional form of the saturated crossover function does not perfectly thread the data, leading to an increased computed error.

Clearly the system is not in the saturated regime over the observed temperature range. However, the saturated crossover function data become a better match to the WL data as T decreases. It seems reasonable that an interpolating crossover function between the saturated and unsaturated crossover functions could be necessary. If an unsaturated/saturated transition is at work, the coherence lengths extracted via a correctly derived interpolating crossover function could agree with those inferred from WL for all temperatures. A definitive test of this hypothesis is to measure TDUCF and MFUCF in extremely thin Ag samples down to dilution refrigerator temperatures and compare their magnitudes and correlation fields. These attempts are ongoing.

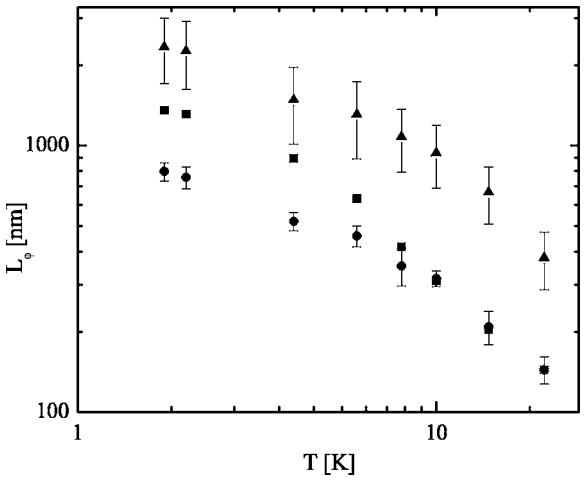

FIG. 5. Coherence lengths from sample F. Squares are from WL, circles are inferred via the unsaturated TDUCF crossover function, and triangles are calculated with the saturated TDUCF crossover function.

C. Drive dependence of the TDUCF

We have also considered whether the nonequilibrium nature of the transport measurements could result in the discrepancy seen in Fig. 4. As has been discussed extensively in Ref. 38, once a system is driven out of equilibrium, it is a subtle question whether one should expect consistency between, e.g., $L_\phi^{\mathrm{WL}}(T)$, $L_\phi^{\mathrm{TDUCF}}(T)$, and $R(T)$. We have examined the drive dependence of our WL and TDUCF measurements and return to this issue below.

Increasing the measurement current has a significant effect on the measured noise power amplitude long before any change is observed in $R(T)$, $L_\phi^{\mathrm{WL}}(T)$, or $L_\phi^{\mathrm{TDUCF}}(T)$. This was seen previously in quasi-2D Ag films.[10] A plot of noise power versus applied current is given in Fig. 6 for several different temperatures. It is clear that the noise power begins to drop at a different applied current for each temperature.

We reemphasize that while the TDUCF amplitude is strongly affected by drive level, the *field-dependence* used to infer L_ϕ^{TDUCF} is essentially unchanged (within the error bars) below drive levels where heating is clearly manifest. Figure 7 shows the experimentally observed noise crossover data for sample J at 2 K for three different drive currents. The left inset indicates that the noise power amplitude shows a distinct drive current dependence while the crossover field of the three curves remains *unchanged* (within the error bars). Over the same range of drive currents, neither L_ϕ^{TDUCF} or L_ϕ^{WL} are altered, to within the error bars on those quantities. This result implies that the coherence length differences observed in the Ag samples [as in Fig. 4(b)] are *not* a result of the type of out-of-equilibrium dephasing effects described in Ref. 38.

A reasonable explanation for the decrease in TDUCF amplitude with increasing drive current is energetic ensemble averaging as eV_c becomes larger than the correlation energy of the samples. As T is increased, the decrease in L_ϕ and

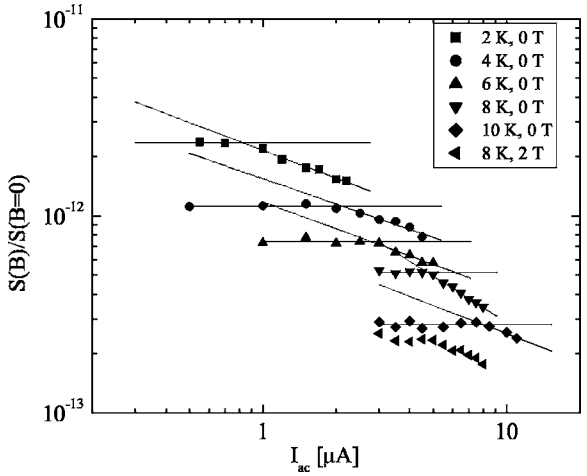

FIG. 6. Sensitivity of the noise power of sample E to applied current. Enhanced suppression of the noise occurs when eV_c becomes larger than the correlation energy. The drop-off current at 8 K, 2 T is the same as 8 K, 0 T implying that the coherence length is not sensitive to large applied fields.

corresponding increase in E_c would require larger drives to observe such averaging, consistent with what is observed. The inability to observe such a suppression of noise at high drives in the AuPd samples, where L_ϕ is much shorter, further supports this explanation. An estimate of the current required such that $eV_c \sim E_c$ in AuPd leads to a current greater than that needed empiricially to heat the samples significantly.

The detailed above-threshold dependence of the noise power on the applied current, however, is surprising. Properly normalized noise power is not proportional to $1/I_{ac}$

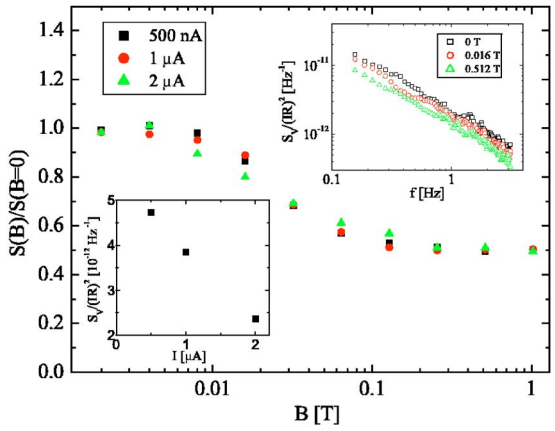

FIG. 7. (Color online) Normalized noise power of sample J at 2 K as a function of field for three different values of drive current (rms 500 nA, 1 μA, and 2 μA). The unchanging crossover field demonstrates explicitly that the inferred L_ϕ^{TDUCF} is *not* affected strongly by drive level. Left inset: dimensionless conductance noise power as a function of drive current at zero field, showing that the higher drive currents do suppress the *magnitude* of the TDUCF. Right inset: log-log plot of the normalized noise power as a function of frequency at 2 K, 2 μA drive, for three different values of B, showing the $1/f$ dependence typical for all the TDUCF data in this work.

above the critical current where $e \times I(R/L)L_\phi \sim E_c$, as a simple treatment would predict. Instead the noise power decreases like $I_{ac}^{-0.5}$ above the threshold. For completeness, the drive dependence at 8 K was repeated at 2 T. The suppression of the noise amplitude started at the same threshold drive current, further evidence that the coherence length in Ag does not change at high fields (i.e., dephasing in Ag is not magnetic impurity scattering in origin).

D. Dephasing mechanisms

The L_ϕ^{WL} and L_ϕ^{TDUCF} data have implications for the decoherence mechanisms at work in these materials. As we argue below, the data strongly support that magnetic impurity scattering is relevant in AuPd samples, and that scattering from dynamical defects such as tunneling two-level systems (TLS) are unlikely to be significant in these materials.

We first consider AuPd, in which the L_ϕ values at low temperatures are significantly lower than those predicted from Nyquist scattering. Exact quantitative agreement between the theoretical Nyquist length and experimental coherence length is not necessarily expected since AuPd is not a simple metal, i.e., it does not have the typical spherical Fermi surface. However, if the Nyquist dephasing mechanism is at work, one should expect that the experimental coherence lengths at low temperature would show the predicted power law dependence with the temperature. Deviations from this power law are particularly clear as apparent low-T saturation of L_ϕ in samples C and D, shown in more detail in Ref. 24.

These deviations are due at least in part to detectable concentrations of magnetic impurities in all AuPd samples. The presence of such impurities is strongly supported by high magnetic field noise power data. Figure 8(a) shows the normalized noise power versus applied field up to 8 T for three samples, the AuPd sample intentionally contaminated with magnetic impurities (D), one nominally clean AuPd sample (C), and one Ag sample (F). A noticeable upturn in the noise power at high fields is seen in both AuPd samples, while no such upturn is seen in the Ag at the lowest measured temperature.

The upturn is caused by a suppression of spin-flip decoherence as the Zeeman splitting of the magnetic impurities exceeds $k_B T$. An analogous upturn has been observed in investigations of Li wires[39] and in recent Aharonov-Bohm measurements in Cu rings.[14] The increased coherence length leads to an increase in the magnitude of the noise power via reduced ensemble averaging. Some upturn is visible at the highest B/T ratio in *all* AuPd samples, consistent with some magnetic impurities even in nominally "clean" devices. Figure 8(b) shows the large field noise upturn at multiple temperatures in sample B. The characteristic field scale for the noise upturn increases with increasing temperature, consistent with Zeeman splitting of magnetic scatterers.

One can use Eq. (11) to estimate the magnetic impurity concentration required to produce the observed L_ϕ saturation values. Assuming that the 2 K data represent complete saturation (as appears to be the case for, e.g., sample C), that $T_K \sim 2$ K, and a typical $\nu(E_F)$ for the noble metals, one finds

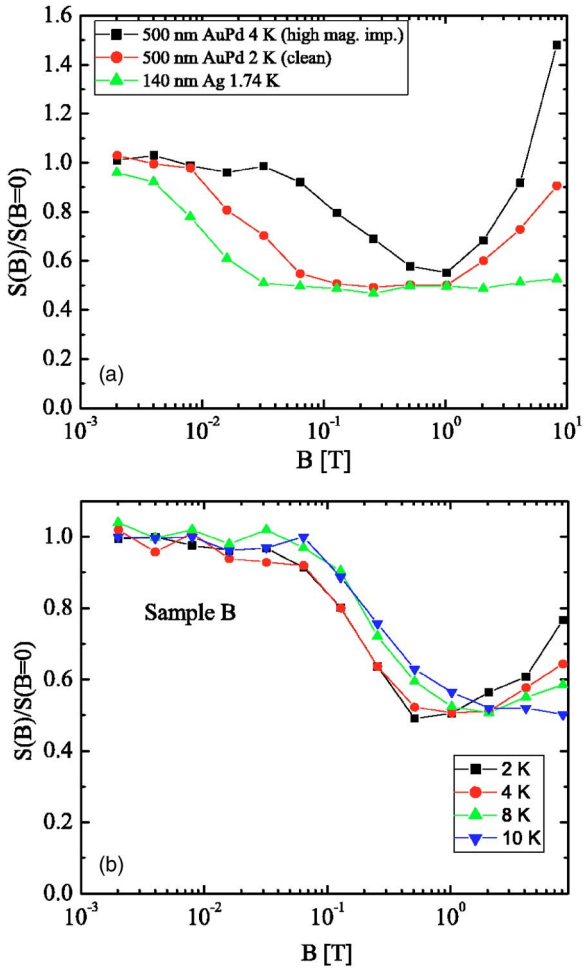

FIG. 8. (Color online) (a) High field noise data for samples C, D, and F, all at 2 K. The upturn at high fields implies that non-negligible concentrations of magnetic impurities exist in the AuPd samples. (b) High field noise data for sample B at several temperatures, showing the upturn in this nominally clean AuPd sample. The lines connecting the points for each temperature are a guide to the eye. Note that the upturn is smaller and happens at higher fields for higher temperatures, consistent with Zeeman splitting of magnetic impurities.

$c_{\mathrm{mag}} \sim 17$ ppm for sample C. This value is surprisingly high and not consistent with the starting purity of the source material. One possible explanation for this would be an enhancement of the spin-flip scattering process due to the strong paramagnetism of the Pd component of the host alloy. Note that even if this concentration of magnetic impurities is accurate, the inferred T^* below which spin-flips should affect UCF and WL differently is <1 K, outside the range of these measurements.

Comparing the saturated values of L_ϕ for two samples allows the *relative* concentrations of magnetic impurities to be computed, independent of possible paramagnetic enhancement or density of states uncertainties, since $c_{\mathrm{mag},2}/c_{\mathrm{mag},1}=D_2/D_1(L_{\phi,1}/L_{\phi,2})^2$. Comparing samples C (quasi-2D) and D (quasi-2D, "spiked" with additional magnetic impurities), one finds that $c_{\mathrm{mag,D}}/c_{\mathrm{mag,C}} \approx 5$. We note that $R(T)$ for these two samples shows no discernable difference beyond what would be expected from their diffusion constants. This also supports the hypothesis that the absolute concentration above is an *overestimate*, since $\sim$100 ppm magnetic impurities in sample D would likely cause other discernable effects in addition to enhanced dephasing. Furthermore, at such a concentration the crossover temperature $T^* \sim 4$ K; however, no change in L_ϕ^{WL} vs L_ϕ^{TDUCF} is apparent there, again suggesting that this concentration is an overestimate.

While the above data show that spin-flip scattering is definitely relevant in AuPd samples, unconventional (non-Nyquist, non-spin-flip) dephasing must also be considered as an alternative explanation for the suppression of low-T coherence lengths as compared to those expected from Nyquist theory. Coherence lengths inferred via WL in Ag samples (G and H) in dilution refrigerator measurements show some evidence of saturation at temperatures much less than 1 K. (Other Ag samples were not measured at dilution temperatures, and clearly had not saturated down to 1.7 K.) The cause of this saturation cannot be dismissed easily as spin-flip scattering at this stage, since we have yet to perform measurements (e.g., TDUCF, Aharonov-Bohm) that would directly probe for magnetic impurities in these samples at those temperatures.

Another proposed mechanism put forth to explain observed coherence saturation is a dephasing mechanism caused by the same dynamic two-level systems that cause TDUCF.[40,41] The data presented herein imply that such a mechanism is unlikely to be the cause of the coherence saturation seen in the AuPd. Using the TDUCF noise amplitude of the two materials at a given temperature, it is possible to use the results of Feng, Lee, and Stone[16] and the measured sample parameters to estimate the ratio of TLS in the two materials. If the microscopic scattering properties of the TLS are assumed to be identical in AuPd (sample A) and Ag (sample J), using the appropriately normalized TDUCF magnitude at 2 K, we find that the density of TLS is $\sim$ three times larger in Ag than in AuPd. This number should be considered a rough estimate since the scattering cross sections of the TLS in the two materials may be different. A conclusion that the mobile defect density is roughly the same in both materials is reasonable. If TLS-induced dephasing truly is significant in AuPd at $\sim$2 K, one would therefore expect it to be similarly important in Ag samples. Given the excellent agreement at that temperature of L_ϕ^{WL} in Ag with the Nyquist prediction, this seems unlikely.

For completeness, we compare maximum (lowest T) coherence times observed for both AuPd and Ag with a prediction of zero temperature coherence time saturation.[42] The predicted zero-temperature dephasing time is

$$\frac{1}{\tau_{\phi,\mathrm{sat}}} = \frac{\sqrt{2}\rho e^2}{3h\pi\sqrt{D}}\left(\frac{b}{\tau_e}\right)^{3/2}. \tag{12}$$

Here, τ_e is the elastic relaxation time of the conduction electrons, ρ is the resistivity, and b is a constant of order one. Since a strict value for b is not known, we select one sample as a reference and compare the ratio of each maximum L_ϕ^{WL} to the ratio expected from Eq. (12) and the measured resis-

TABLE I. Samples used in magnetotransport and noise measurements. Free electron density of states for Au and Ag used to calculate D for AuPd and Ag samples: 1×10^{47} m^{-3} J^{-1}, from Ref. 43. Diffusion constants calculated via the Einstien relations. Sample D was deliberately contaminated with additional ferromagnetic impurities as described in the text. The effective dimensionality d for coherence effects is determined by the relative size of L_ϕ and the sample dimensions.

Sample	Metal	d	w [nm]	t [nm]	R/L [Ω/μm] (1D) $R/\square$ [Ω] (2D)	D [m^2/s]
A	AuPd	1	43	9	722	1.34×10^{-3}
B	AuPd	1	35	9	857	1.34×10^{-3}
C	AuPd	2	500	6.5	84.5	7.9×10^{-4}
D	AuPd	2	500	8.5	47.5	9.6×10^{-4}
E	Ag	1	115	12	49	5.65×10^{-3}
F	Ag	1	140	12	35	6.70×10^{-3}
G	Ag	1	130	12	45	5.63×10^{-3}
H	Ag	1	70	20	42	6.50×10^{-3}
I	Ag	1	125	12	43	5.91×10^{-3}
J	Ag	1	100	12	88.5	3.61×10^{-3}

tivities. We acquired WL data on Ag samples G and H in the dilution refrigerator, with some indications of L_ϕ^{WL} saturation; for AuPd samples C and D, such saturation has an onset at temperatures above 2 K. Since the Ag shows the least magnetic contamination, we choose sample H as the reference (see Table I). In Table II we show the predicted ratios from applying Eq. (12), which fall well outside the errors in the experimentally measured ratios for two of the three samples. In fact, the one sample that shows good agreement with Eq. (12) is sample D, the sample intentionally contaminated with *additional* magnetic impurities known to significantly impact coherence. These data do not appear to support Eq. (12). Given the demonstrated effectiveness[12] of trace magnetic impurities to affect L_ϕ^{WL}, one must view analyses of low temperature coherence saturation with appropriate caution.

TABLE II. L_ϕ^{WL}(max) normalized by that for sample H, compared with the expected ratio from Eq. (12) for zero-temperature saturation of τ_ϕ, using sample parameters from Table I.

Sample ratio	Measured	Uncertainty	Expected
C/H	0.0597	0.0017	0.0148
D/H	0.0221	0.0006	0.0218
G/H	0.6561	0.0186	0.7502

V. CONCLUSION

We have performed detailed measurements of the WL magnetoresistance, TDUCF amplitude as a function of field, and the magnetofingerprint of both AuPd and Ag mesoscopic wires. A comparison of the coherence lengths inferred from WL and TDUCF measurements are in strong quantitative agreement for the AuPd samples while a disagreement was observed in the Ag samples similar to that previously seen in Ag films. We hypothesize that the reason for this discrepancy is that Ag may be approaching the saturated noise limit, and further experiments to test this are ongoing. The observed suppression of TDUCF magnitude at high drive currents in Ag agrees qualitatively with ensemble averaging related to the correlation energy scale, though a quantitative understanding is still lacking. Finally, we have considered the coherence saturation seen in our quasi-2D AuPd samples, and discussed the important influence of magnetic impurities in such systems. The subtle physics, rich phenomenology, and continued presence of surprises (such as the disagreement between WL and TDUCF in Ag) demonstrate why electronic coherence in solids remains a lively area for investigation.

ACKNOWLEDGMENTS

We would like to thank N. O. Birge for his helpful advice concerning noise measurements, and I. L. Aleiner and A. D. Stone for discussions of the theory. This work was supported by DOE Grant No. DE-FG03-01ER45946/A001 and the David and Lucille Packard Foundation.

[1] Y. Imry, *Introduction to Mesoscopic Physics* (Oxford University Press, Oxford, 1997).
[2] W. J. Liang, M. Bockrath, D. Bozovic, J. H. Hafner, M. Tinkham, and H. Park, Nature (London) **411**, 665 (2001).
[3] F. Capasso, J. Faist, and C. Sirtori, J. Math. Phys. **37**, 4775 (1996).
[4] G. Bergmann, Phys. Rep. **107**, 1 (1984).
[5] W. J. Skocpol, P. M. Mankiewich, R. E. Howard, L. D. Jackel, D. M. Tennant, and A. D. Stone, Phys. Rev. Lett. **56**, 2865 (1986).
[6] S. Washburn and R. A. Webb, Rep. Prog. Phys. **55**, 1311 (1992).
[7] N. O. Birge, B. Golding, and W. H. Haemmerle, Phys. Rev. Lett. **62**, 195 (1989).
[8] N. Giordano, in *Mesoscopic Phenomena in Solids*, edited by B. L. Altshuler, P. A. Lee, and R. A. Webb (Elsevier, New York, 1991), p. 131.
[9] R. A. Webb, S. Washburn, C. P. Umbach, and R. B. Laibowitz, Phys. Rev. Lett. **54**, 2696 (1985).
[10] D. Hoadley, P. McConville, and N. O. Birge, Phys. Rev. B **60**, 5617 (1999).
[11] P. Mohanty, E. M. Q. Jariwala, and R. A. Webb, Phys. Rev. Lett. **78**, 3366 (1997).
[12] F. Pierre, A. B. Gougam, A. Anthore, H. Pothier, D. Esteve, and N. O. Birge, Phys. Rev. B **68**, 085413 (2003).
[13] D. S. Golubev and A. D. Zaikin, Phys. Rev. Lett. **81**, 1074 (1998).
[14] F. Pierre and N. O. Birge, Phys. Rev. Lett. **89**, 206804 (2002).
[15] P. Mohanty and R. A. Webb, Phys. Rev. Lett. **91**, 066604 (2003).
[16] S. Feng, P. A. Lee, and A. D. Stone, Phys. Rev. Lett. **56**, 1960 (1986); **56**, 2772(E) (1986).
[17] A. D. Stone, Phys. Rev. B **39**, 10736 (1989).

[18] P. A. Lee and A. D. Stone, Phys. Rev. Lett. **55**, 1622 (1985).
[19] B. L. Altshuler and D. E. Khmelnitskii, JETP Lett. **42**, 359 (1986).
[20] A. D. Stone, Phys. Rev. Lett. **54**, 2692 (1985).
[21] *Tunneling Systems in Amorphous and Crystalline Solids*, edited by P. Esquinazi (Springer-Verlag, New York, 1998).
[22] Ya. M. Blanter, Phys. Rev. B **54**, 12807 (1996).
[23] I. L. Aleiner and Ya. M. Blanter, Phys. Rev. B **65**, 115317 (2002).
[24] A. Trionfi, S. Lee, and D. Natelson, Phys. Rev. B **70**, 041304(R) (2004).
[25] J. H. Scofield, Rev. Sci. Instrum. **58**, 985 (1987).
[26] J. J. Lin and N. Giordano, Phys. Rev. B **35**, 1071 (1987).
[27] I. L. Aleiner (private communication, 2003).
[28] P. A. Lee, A. D. Stone, and H. Fukuyama, Phys. Rev. B **35**, 1039 (1987).
[29] N. O. Birge, B. Golding, and W. H. Haemmerle, Phys. Rev. B **42**, 2735 (1990).
[30] C. W. J. Beenakker and H. van Houten, Phys. Rev. B **37**, R6544 (1988).
[31] V. Chandrasekhar, P. Santhanam, and D. E. Prober, Phys. Rev. B **42**, R6823 (1990).
[32] P. McConville and N. O. Birge, Phys. Rev. B **47**, R16667 (1993).
[33] P. Dutta and P. M. Horn, Rev. Mod. Phys. **53**, 497 (1981).
[34] J. Pelz and J. Clarke, Phys. Rev. B **36**, R4479 (1987).
[35] S. Hershfield, Phys. Rev. B **37**, 8557 (1988).
[36] C. Van Haesendonck, J. Vranken, and Y. Bruynseraede, Phys. Rev. Lett. **58**, 1968 (1987).
[37] S. Feng, in *Mesoscopic Phenomena in Solids*, edited by B. L. Altshuler, P. A. Lee, and R. A. Webb (Elsevier, New York, 1991), p. 107.
[38] Z. Ovadyahu, Phys. Rev. B **63**, 235403 (2001).
[39] J. S. Moon, N. O. Birge, and B. Golding, Phys. Rev. B **56**, 15124 (1997).
[40] A. Zawadowski, J. von Delft, and D. C. Ralph, Phys. Rev. Lett. **83**, 2632 (1999).
[41] Y. Imry, H. Fukuyama, and P. Schwab, Europhys. Lett. **47**, 608 (1999).
[42] D. S. Golubev, A. D. Zaikin, and G. Schön, J. Low Temp. Phys. **126**, 1355 (2002).
[43] N. W. Ashcroft and N. D. Mermin, *Solid State Physics* (Hold, Rinehart, and Winston, New York, 1976).